Jour. Korean Inst. Mining Geol.
Vol. 19, No. 3, p. 199-218, 1986

Compositional Variation of Arsenopyrites in Arsenic and Polymetallic Ores from the Ulsan Mine, Republic of Korea, and their Application to a Geothermometer*

Seon-Gyu Choi, Jae-Ill Chung** and Naoya Imai****

Abstract: Arsenopyrite in arsenic and polymetallic ores from calcic Fe-W skarn deposit of the Ulsan mine, Republic of Korea, has been investigated by means of electron microprobe analysis and X-ray diffractometry. As a result, it is revealed that the Ulsan arsenopyrite may be classified into the following three species with different generation on the basis of its mode of occurrence, chronological order during polymetallic mineralization and chemical composition; arsenopyrites I, II and III.

1) Arsenopyrite I—(Ni, Co)-bearing species belonging to the oldest generation, which has crystallized together with (Ni, Co)-arsenides and -sulpharsenides in the early stage of polymetallic mineralization. In rare cases, it contains a negligible amount of antimony. It occurs usually as discrete grains with irregular outline, showing rarely subhedral form, and is diffused in skarn zone. The maximum contents of nickel and cobalt are 10.04 Ni and 2.45 Co (in weight percent). Occasionally, it shows compositional zoning with narrow rim of lower (Ni+Co) content.

2) Arsenopyrite II—arsenian species, in which (Ni+Co) content is almost negligible, may occur widely in arsenic ores, and its crystallization has followed that of arsenopyrite I. It usually shows subhedral to euhedral form and is closely associated with löllingite, bismuth, bismuthinite, chalcopyrite, sphalerite, bismuthian tennantite, etc. It is worthy of note that arsenopyrite II occasionally contains particles consisting of both bismuth and bismuthinite.

3) Arsenopyrite III—(Ni, Co)-free, S-excess and As-deficient species is close to the stoichiometric composition, FeAsS. It occurs in late hydrothermal veins, which cut clearly the Fe-W ore pipe and the surrounding skarn zone. It shows euhedral to subhedral form, being extremely coarse-grained, and is closely associated with pyrite, "primary" monoclinic pyrrhotite, galena, sphalerite, etc.

Among three species of the Ulsan arsenopyrite, arsenopyrite I does not serve as a geothermometer, because (Ni+Co) content always exceeds 1 weight percent. In spite of the absence of Fe-S minerals as sulphur-buffer assemblage, the presence of $Bi(l)$-Bi_2S_3 sulphur-buffer enables arsenopyrite II to apply successfully to the estimation of either temperature and sulphur fugacity, the results are, $T=460\sim470°C$, and $\log f(S_2)=-7.4\sim-7.0$. With reference to arsenopyrite III, only arsenopyrite coexisting with pyrite and "primary" monoclinic pyrrhotite may serve to restrict the range of both temperature and sulphur fugacity, $T=320\sim440°C$, $\log f(S_2)=-9.0\sim-7.0$. These temperature data are consistent with those obtained by fluid inclusion geothermometry on late grandite garnet somewhat earlier than arsenopyrite II.

At the beginning of this paper, the geological environments of the ore formation at Ulsan are

* Presented at the Autumn Joint Meeting of the Society of Mining Geologists of Japan, Japanese Association of Mineralogists, Petrologists and Economic Geologists and the Mineralogical Society of Japan, held in Kumamoto University on Sept. 29, 1985.

** Department of Mineral Industry, School of Science and Engineering, Waseda University, Japan Present address of S.G. Choi: Department of Earth Science Education, Korea National University of Education, Korea.

considered from regional and local geologic settings, and physicochemical conditions are suspected, in particular the formation pressure (lithostatic pressure) is assumed to be 0.5kb (50MPa). The present study on arsenopyrite geothermometry, however, does not bring about any contradictions against the above premises. Thus, the following genetical view on the Ulsan ore deposit previously advocated by two of the present authors (Choi and Imai) becomes more evident; the ore deposit was formed at shallow depth and relatively high-temperature with steep geothermal gradient—xenothermal conditions.

INTRODUCTION

Arsenopyrite widely occurs with varying amounts in many ore deposits of different genesis and has received considerable attention from economic geologists as a geothermometer. The ideal formula of arsenopyrite is FeAsS, however, natural arsenopyrites usually contain small amounts of nickel and cobalt which substitute for iron, and antimony and bismuth substituting for arsenic.

Morimoto and Clark (1961) have shown that arsenic and sulphur in arsenopyrites can be mutually substituted to the limits of $FeAs_{0.9}S_{1.1}$ and $FeAs_{1.1}S_{0.9}$, and concluded that the space group $P1$ approaching $P2/c$ as the arsenic content increases. On the other hand, the recent experimental study for the system Fe-As-S by Kretschmar and Scott (1976) shows that the As/S atomic ratio or atomic percent As in arsenopyrites ($FeAs_{1\pm x}S_{1\pm x}0 \leqq x \leqq 0.1$) is mainly a function of their formation temperatures, only when they come from sulphur-buffer assemblages; e.g., arsenopyrite+pyrite+hexagonal pyrrhotite.

At Ulsan, arsenopyrite is widespread and represents a major constituent in the concentrates of arsenic ores coming from mill plant. In a previous paper (Choi and Imai, 1985), in which Ni-Fe-Co arsenides and sulpharsenides except for arsenopyrite were described, it was pointed out that the Ulsan arsenopyrites might be classified into three species with different generation, designated as arsenopyrites I, II and III on the basis of the chronological order in its crystallization during the course of polymetallic mineralization.

This paper is designed to present compositional variation of the Ulsan arsenopyrites with their mode of occurrence and paragenetic sequence, and finally an attempt is made to decipher the physicochemical environments under which the Ulsan ores have been formed, in particular their formation temperatures utilizing arsenopyrite geothermometer.

GEOLOGIC ENVIRONMENTS OF ORE FORMATION

Location and regional geologic setting

The Ulsan mine is located in Nongso Myeon, Gyeongsangnam-Do Province, Republic of Korea (lat. 35° 37'N and long. 129° 20' E), lying about 10km north from the centre of Ulsan City. The calcic Fe-W skarn deposit of this mine represents an important producer of iron, tungsten and arsenic ores in this country.

Geotectonically, the mine area lies within the southeastern border of the Gyeongsang sedimentary basin, which occupies the southeastern part of the Korean peninsula. The Gyeongsang Supergroup, about 9,000m thick, which is unconformably underlain by the highly-deformed sequence of the Precambrian crystalline basement in the Ryeongnam massif. Igneous activity of the Daebo Intrusive Suite has prevailed during Jurassic time in this massif.

Sedimentary piles in the basin are dominantly

nonmarine, having been deposited under lucustrine and fluviatile environments during Cretaceous time, and are divided into three stratigraphic units; the Lower Cretaceous Sindong Group, the Middle Cretaceous Hayang Group, and the Upper Cretaceous Yucheon Group. The Sindong Group consists of nonmarine sedimentary rocks and is conformably overlain by the Hayang Group, which is also a sequence of sedimentary rocks with minor intercalations of volcanic horizon.

The Yucheon Group is dominantly composed of volcanic rocks ranging in composition from intermediate to felsic, and rests unconformably upon both the Hayang and Sindong Groups (Chang 1975).

The volcanic rocks of calc-alkaline affinities appear to be predominate in the Yucheon Group, which is exposed mainly in the southeastern part of the basin (Milyang block), where andesitic pyroclastics and lava flows tend to be overlain by felsic lapilli-, lithic- and ash-flow tuffs (Chang, 1975).

The Bulgugsa Intrusive Suite within the basin, the age of which ranges from the Middle Cretaceous to Early Paleogene, consists of granitic rocks, varying in composition from tonalite and granodiorite to alkali-feldspar granite through granite, which are predominantly magnetite-series granitoids (Ishihara et al., 1981), and occupies about a quarter surface area in the basin. Among them, the rocks with granitic composition are most predominate in quantity. The granitic rocks within the basin invariably display characteristics indicating their epizonal, subvolcanic emplacement (Jin et al., 1981; Imai and Choi, 1984). The Bulgugsa Intrusive Suite and the volcanic horizons of the Hayang and Yucheon Groups are believed to be comagmatic. These volcano-plutonic complexes are considered to have been generated in the subduction zones at a convergent plate margin (e. g., Sillitoe, 1980).

Jin et al. (1981) have concluded that the mineralization associated with volcano-plutonism in the Gyeongsang basin appears to be controlled by "circular" structure (dome structure) resulted from the subvolcanic emplacement of the granitic magma following subaerial or terrestrial volcanism therein.

Local geologic setting

Over the Ulsan Quadrangle (Geologic Map, 1/50,000 in scale with Explanation Text; Park, Y.D. and Yoon, H.D., 1968), called "Ulsan district" in the present paper, where Ulsan mine area occupies the southwestern portion, widely exposed are sedimentary rocks of the Ulsan Group, the overlying volcanic accumulation of the Chisulryeong and Yucheon Volcanic Complexes, and the plutons of the Bulgugsa Intrusive Suite.

The Ulsan Group that is correlative broadly with the Hayang Group has been divided into the following three formations in ascending order; the Guyeonri Formation, the Sayeonri Formation and the Joilri Formation. The Guyeonri Formation crops out in the restricted areas, western part of Ulsan City, and is dominantly composed of black shale or mudstone of lucustrine origin. This formation is gradational into the overlying Sayeonri Formation. Although the base is hidden, the thickness is assumed to be about 800 m (Choi, et al, 1980). The Sayeonri Formation covers about eighty percent of the Ulsan district. It consists largely of purplish mudstone with minor amounts of sandstone and pebbly sandstone of flood plain origin. It is about 2,500 m thick, as suggested by Choi, et al. (1980). At the Ulsan mine, the base of this formation is represented by the volcanic horizon of trachyandesite (Choi, 1983), called quartz latite by Park and Park (1980). The Joilri Formation crops out in the southeastern portion of the Ulsan City, and is composed of dark grey mudstone and calcareous mudstone of lucustrine

origin. The thickness is assumed to be about 750 m, although its upper limit is unknown.

The Chisulryeong Volcanic Complex exposed mainly in the northwestern area of the Ulsan district, consists of welded-, crystal-, lapilli-tuffs and intrusives of felsic composition. In the environs of the Ulsan mine, rhyolite intrudes into the rocks of the Ulsan Group and is intruded by the comagmatic hornblende-biotite granite ("Gadaeri granite pluton").

The Yucheon Volcanic Complex is distributed in the western part of the Ulsan district in the form of both intrusive and extrusive, and composed of lava flow, tuffaceous agglomerate and volcanic breccia of felsic composition. The sequence of this complex is also intruded by the comagmatic granitic rocks.

In the Ulsan district, Tertiary sediments and volcanics are distributed in the restricted areas, but their description is omitted here, because they have no relations to the ore-forming event.

In the Ulsan mine area, there is narrow "island" with oval shape on the surface, consisting of thermally metamorphosed ultramafic rocks (dunite~harzburgite in mineral composition) partly serpentinized (Choi, 1983; Choi and Imai, 1985) and limestones (calcite-marbles) that are the host rocks of the Fe-W mineralization. This "island" is surrounded perfectly by the rocks of the Sayeonri Formation and the intruded granitic rocks, occupying the centre of dome structure called "Gadaeri granite pluton", the K/Ar age of which is 58 Ma on biotite (Lee and Ueda, 1977). Though the age of both ultramafic rocks and limestones is unknown, they are considered to represent the basement rocks of the Cretaceous sediments (Park and Park, 1980; Choi et al., 1983; Choi, 1983).

The exposure of basement rocks occurring as an "island" within the "sea" of the Gyeongsang basin may be explained probably by the marked palaeo-topographic relief of the basement at the initial stage of deposition of the Sayeonri Formation as well as by the subsequent uplift of west side of Ulsan fault that trends north-northwest in general, running through the immediate east of the Ulsan mine.

The Ulsan ore deposit accompanied with calcic skarn is represented by an ore pipe dominatly composed of magnetite with lesser amounts of scheelite which is distributed pervasively in northern portion of the ore pipe. Formation of this ore pipe appears to be controlled structurally by the intersections of two structural elements; i.e., (1) east-west trending and steeply dipping stratigraphical contact between limestones and the overlying Cretaceous sediments with an intercalation of volcanic rocks (trachyandesite), and (2) north-south trending high-angle fractures now occupied by swarms of post-ore andesitic dykes. In spite of the spatial separation of the mineralized zones from "Gadaeri granite pluton", the ore deposit has been considered to have genetically intimate relation to the intrusive activity of the pluton (Park and Park, 1980; Choi et al., 1983; Choi, 1983).

Pressure estimation

As will be mentioned in the forecoming chapter, sphalerite from the Ulsan mine does not serve as a geobarometer. Accordingly, the (lithostatic) pressure at the time of ore deposition must be suspected from other modes of estimation. The formation pressure at Ulsan is the most difficult intensive variable as in case of ore deposits elsewhere.

Choi (1983) has already proposed a value of the formation pressure at about 0.5 kb (50 MPa) for the Ulsan ore deposit. This is based upon the assumption that the mineralization related to the intrusive activity of "Gadaeri granite pluton" has taken place at about 58 Ma ago (Tantian stage) and that depth of base of the Sayeonri Formation, around which the mineralization has taken place, is approximately equi-

valent to its stratigraphic thickness of about 2,500 m given by Choi et al. (1980), taking pre-date erosional processes into account.

The maximum depth of mine workings and bore holes outlining orebody at Ulsan is only 250 m, which may be almost negligible. The overburden thickness of 2,500 m corresponds to maximum pressure at about 0.7 kb(70 MPa).

"Gadaeri granite pluton" with circular shape of about 6 km in diameter, consists of equigranular hornblende-biotite granite in the core, but towards the intrusive contact the development of porphyritic structure together with myrmekitic and micrographic textures become conspicuous, and phenocryst of plagioclase (An_{20}–An_{30}) is a high-temperature type showing commonly oscillatory zoning. Moreover, the pluton is surrounded by a contact-metamorphic aureole, and the mineralization at Ulsan shows a steep geothermal gradient (Choi, 1983; Imai and Choi, 1984). These facts clearly indicate its emplacement of high-level types. Summarizing the statements as noted above, the value of 0.5 kb (50MPa) seems reasonable as a formation pressure therein.

PROBLEMS ON SPHALERITE GEOBAROMETRY

Scott and Barnes(1971) showed that the composition of sphalerite (FeS content in ZnS) might serve as a useful geobarometer, provided that sulphur fugacity was buffered with pyrite+hexagonal pyrrhotite. Since then, several authors have tested for some ore deposits (e. g., De Witt and Essene, 1974; Berglund and Ekstrom, 1980; Lusk et al., 1975; Imai and Lee, 1980; Shimizu and Shimazaki, 1981). In many cases, however, the sphalerite geobarometry seems to give anomalous values, showing unexpectedly high pressure except a few successes. Recently Scott (1983) has pointed out that sphalerite is applicable to a geobarometer only when the ore specimens were subjected to sufficiently rapid cooling to prevent from retrograde reaction.

In the Ulsan polymetallic ores, sphalerite commonly occurs as an important constituent, though minor in amount, however, it does not serve as a geobarometer, and the reason why this is so will be described below. As shown in Fig. 1, which will appear later, the Ulsan sphalerite may be classified into two species with distinctly different generation on the basis of its mode of occurrence and chronological order; sphalerites I and II.

Sphalerite I is a product in stage IIb, having crystallized earlier during skarn growth, and characterized by the low iron content (0.3～0.5 mole percent FeS). It is closely associated with arsenopyrite II, chalcopyrite, bornite, bismuth and bismuthinite. Sphalerite I accompanied by roquesite ($CuInS_2$) contains appreciable amounts of indium and copper; up to 2.11 In and 1.27 Cu (all in weight percent) (Imai and Choi, 1984). On the other hand, sphalerite II is a product in stage III, having crystallized during the formation of late hydrothermal veins and characterized by relatively high iron content (14.3～19.6 mole percent FeS). It is intimately intergrown with pyrite, arsenopyrite III and "primary" monoclinic pyrrhotite. No sulphur-buffer assemblages of the Fe-S system have been encountered in both ore types; i. e., the absence of primary hexagonal pyrrhotite.

SKARN EVOLUTION AND METALLIC MINERALIZATION

At Ulsan, metasomatic process of skarn growth in the time-evolutional trend, following the formation of metamorphic skarns ("skarnoids") by thermal metamorphism due to the intrusion of "Gadaeri granite pluton", may be divided broadly into two stages based upon the paragenetic sequence of calc-silicates and their chemical

composition; early and late skarn stages.

Early skarn stage, during which the skarn growth shows prograde step, has started with the formation of highly calcic assemblage, diopsidic clinopyroxene + wollastonite recognized occasionally at the skarn front in calcite-marbles. It is followed by the formation of clinopyroxenes with salite to ferrosalite composition and grandite garnets with grossular-rich composition. This skarn stage is essentially barren of ore minerals (early barren stage). It is well established from the field and microscopic observations, however, that the main Fe-W mineralization that plays an important role for the formation of the ore pipe has taken place at the end of this early skarn stage (Choi and Imai, 1985).

Earlier period of late skarn stage representing progade skarn growth shows a trend towards the enrichment of noticeable iron and slight manganese, and magnesium depletion; clinopyroxenes have hedenbergitic composition and grandite garnets have andraditic composition. On the other hand, later period of this skarn stage is retrograde in which the hydrous alteration of the preexisting skarn minerals has been represented mainly by the alteration of clinopyroxenes into calcic amphiboles, and "neo-formation" of hydrous silicates, carbonates and quartz has been prevailed.

In the later half period of late skarn stage, complex metallic mineralization has proceeded, the majority of which has been superimposed upon the previous Fe-W mineralization; i.e., a large number of metals and semimetals of Mn, Fe, Co, Ni, Cu, Zn, As, Mo, Ag, In, Sn, Sb, Te, Pb and Bi have been fixed in various states, such as sulphides, arsenides, sulpharsenides, sulphosalts and tellurides, although these ore minerals are minor or trace in amounts except for arsenopyrite and löllingite.

The ore mineralogy of the Ulsan ore deposit, especially a study of growth and replacement

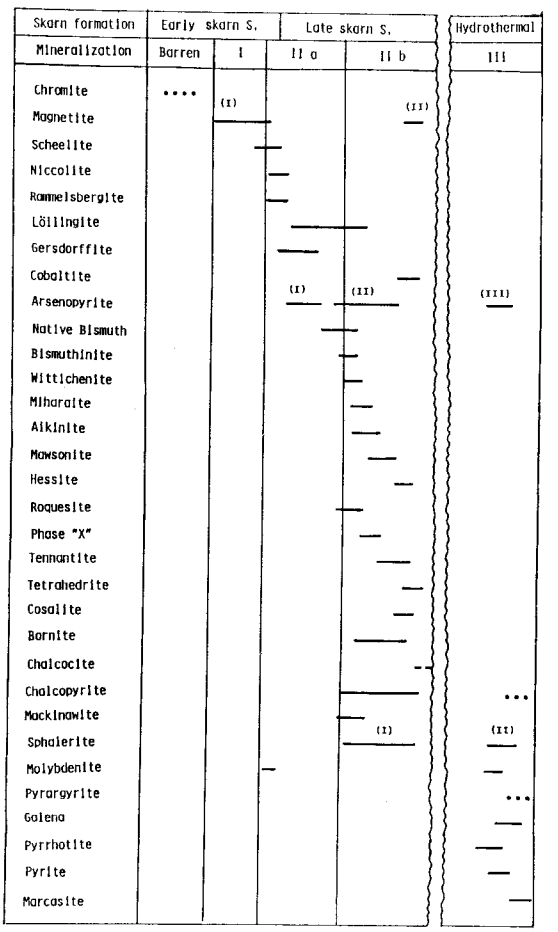

Fig. 1 Paragenetic sequence of ore minerals in the Ulsan ores, somewhat modified after Choi (1983).

textures on the slabs of polymetallic ores has revealed the paragenetic relations of ore minerals attaining more than thirty in number. Figure 1 is a diagrammatic representation showing mineral paragenesis, somewhat modified after Choi (1983), in which skarn stages in relation to metallic mineralization are also illustrated.

As can be seen in Fig. 1, four episodes of hypogene mineralization are recognized and the mineralization may be divided into four distinct stages I, IIa, IIb and III on the basis of chronological order of ore minerals and their chemical composition, and of field relations. Stage IIa and IIb are not interrupted, but successive and must

be regarded as a single mineralization system in late skarn stage, whereas stage III represents the latest phase of hydrothermal mineralization that forms fissure veins and has proceeded after tectonic break (fracturing event) separated perfectly from stage IIb.

Stage I is an initial phase of mineralization that immediately follows early barren stage at Ulsan, during which prominent magnetite (Mt I) deposition and the subsequent scheelite impregnation take place.

Stage IIa has begun with the erratical impregnation of minor or trace amounts of niccolite, rammelsbergite, löllingite I, gersdorffite, arsenopyrite I, (Ni,Co)-bearing species, which is followed by the prominent deposition of löllingite II, (Ni, Co)-free species, and arsenopyrite II, (Ni,Co)-free species; i.e., as a whole early minerals are arsenides and late minerals are sulpharsenides (Choi and Imai, 1985). On the other hand, stage IIb is represented by the crystallization of arsenopyrite II, löllingite II, bornite, chalcocite, (In- and Cu-bearing) sphalerite and bismuthian tennantite with minor or trace amount of bismuth, bismuthinite, roquesite, cobaltite, wittchenite, miharalite, hessite and aikinite; i. e., it is rather characterized by Cu-, Zn- and Bi-minerals (Choi and Imai, 1983a, b, 1985).

Stage III represents the formation of fissure veins, up to 40 cm wide, cutting clearly Fe-W ore pipe and the surrounding wallrocks, a part of which has previously been mineralized. These sharply-defined veins have two different mineral assemblages (1) pyrite + galena + sphalerite + arsenopyrite III + chalcopyrite + tetrahedrite + pyrargyrite + marcasite (gangue mineral: siderite) found in ores of Type D_1 and (2) "primary" monoclinic pyrrhotite + arsenopyrite III + sphalerite + chalcopyrite + molybdenite in ores of Type D_2 in Table 1. Time relation between these two kinds of vein is unknown, because they are separated in space.

Table 1 Ore and skarn specimens from the Ulsan mine, subjected to a close examination.

Specimen No.	Occurrence site	Type	Mineral assemblage
US-101	Open pit (bench, 40m above sea level)	Massive(B)	ap-bi-bm
106	Open pit (bench, 35m above sea level)	Massive(B)	ap-bi-bm
112	Open pit (bench, 50m above sea level)	Disseminated(A)	cm-ap-mt-nc-rm-cp
316	−60m adit level	Massive(B)	ap-gf-mo-bi-lo
338	−60m adit level	Disseminated(A)	gf-nc-cm-ap-cp-rm-lo
532	−110m adit level	Disseminated(A)	ap-gf-nc-cp-lo-rm
600	−110m adit level	Late vein(D_1)	py-gl-sp-mc-ap-cp-td-pg
709	−225m adit level	Late vein(D_2)	po-ap-sp-cp-mo
733	−225m adit level	Disseminated(B)	mt-lo-ap-bi
807	−225m adit level	Massive(B)	ap-bi
820880	−225m adit level	Massive(B)	mt-sh-cp-ap-lo-cb-bo-bi-td-rq-cs-mk
1022	−225m adit level	Massive(B)	ap-lo-bi
B8004-4	Boring core	Late vein(D_1)	py-gl-sp-mc-ap-cp
B8102-2	Boring core	Massive(B)	ap-lo-bi
B8103-3	Boring core	Disseminated(B)	ap-bi

Abbreviations; ak=aikinite, ap=arsenopyrite, bi=bismuth, bm=bismuthinite, bo=bornite, cb=cubanite, cc=chalcocite, cm=chromite, co=cobaltite, cp=chalcopyrite, cs=cosalite, gf=gersdorffite, gl=galena, hs=hessite, lo=löllingite, mc=marcasite, mh=miharaite, mk=mackinawite, mo=molybdenite, mt=magnetite, mw=mawsonite, nc=niccolite, pg=pyrargyrite, po=pyrrhotite, py=pyrite, rm=rammelsbergite, rq=roquesite, sh=scheelite, sp=sphalerite, td=tedrahedrite, tn=tennantite, wi=wittichenite.

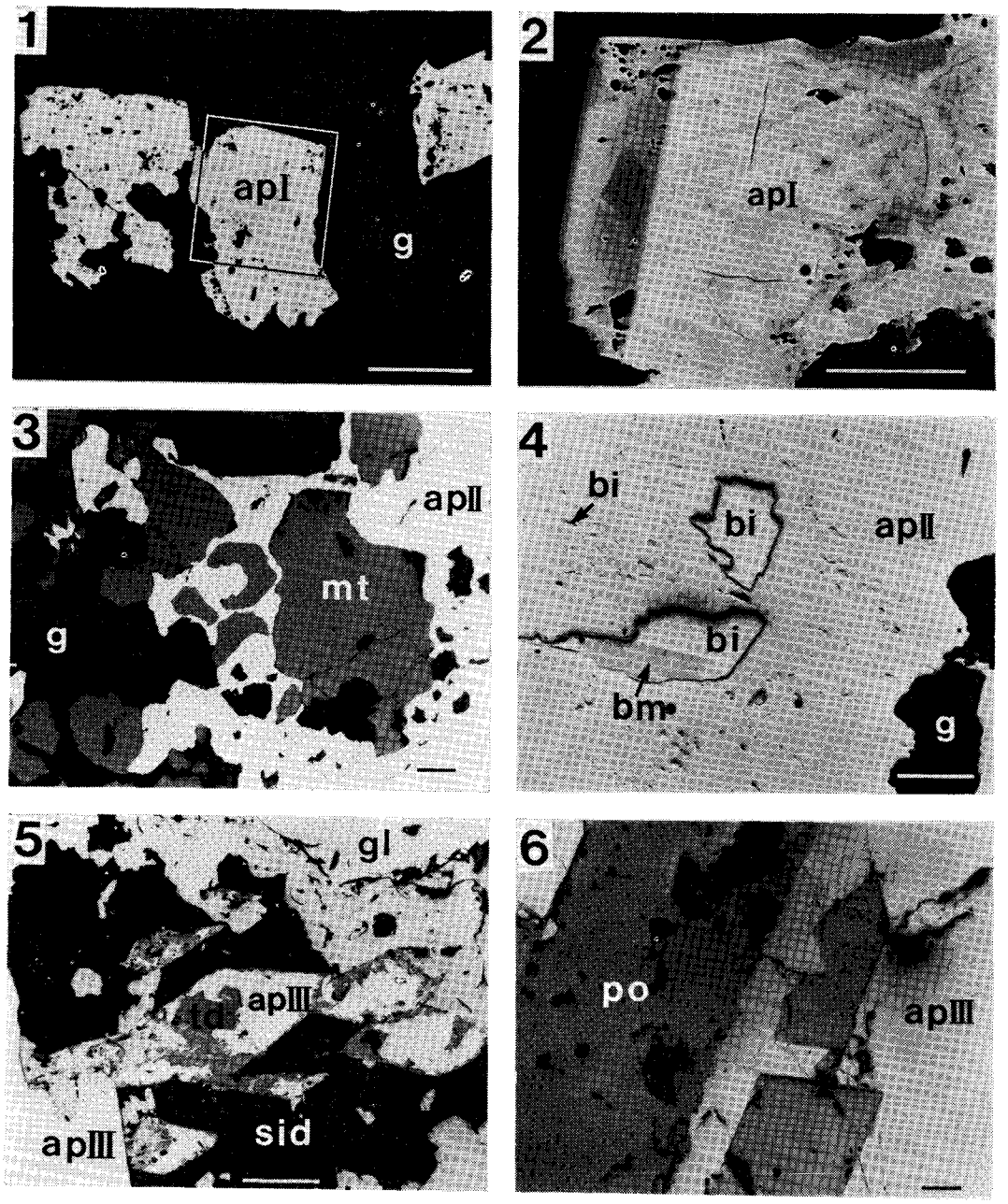

Fig. 2 Photomicrographs and back-scattered electron image of polished sections, showing the mode of occurrence and compositional zoning of arsenopyrites from the Ulsan mine.
(1) and (3)~(6): photomicrographs in reflected light, bar scale indicates 100μm in length; (2): back-scattered electron image, bar scale indicates 50μm in length, the field corresponds to the rectangle marked in (1).
Specimens; (1) and (2): US-532, (3): US-733, (4): US-106, (5): US-600, (6): US-709.
Abbreviations; ap I=arsenopyrite I, ap II=arsenopyrite II, ap III=arsenopyrite III, bi=bismuth, bm =bismuthinite, g=gangue minerals (skarn minerals and calcite), gl=galena, mt=magnetite I, sid =siderite, td=tetrahedrite.

SKARN AND ORE SPECIMENS EXAMINED

Among about two hundred skarn and ore specimens from the Ulsan mine containing arsenopyrite now under investigation, those subjected to a close examination (fifteen hand specimens) are listed in Table 1, in which their brief description is given. The specimens containing the Ni-Fe-Co arsenides and sulpharsenides involving arsenopyrite may be divided previsionally into four types in terms of their field occurrence, difference in host rocks, physical properties and mineralogy; they are Types A, B, C and D (Choi and Imai, 1985). Among them, ores of Type C do not appear in Table 1, because arsenopyrite is absent in the ores.

MODE OF OCCURRENCE AND OPTICAL PROPERTIES

Arsenopyrite I, (Ni,Co)-bearing species tends to occur as discrete grain with irregular outline, which are erratically distributed in skarn zone. Its grain size is usually 100~200 μm across. Generally, it fills interstices between fine-grained calc-silicate aggregates, consisting commonly of clinopyroxene+grandite garnet + calcic amphibole, belonging to ores of Type A in Table 1. On some occasions, it has the remnants of gersdorffite in its core. There are also euhedral to subhedral rhombs rimmed with the outer layer with lower (Ni,Co)-concentration, though this compositional zoning cannot be recognized optically (Fig. 2 (1)), but is recognizable in the back-scattered electron image (Fig. 2 (2)), as well as in the linear-scanning profiles obtained by electron microprobe traverses and X-ray scanning images from characteristic X-rays as will be shown later (Fig. 6 (A) and (B)).

Arsenopyrite II, arsenian species, occurs widely in arsenopyrite- and/or chalcopyrite-rich massive ores distributedwithin Fe-W ore pipe and in both the surrounding skarn zone and "abnormal calcite zone" (Imai and Choi, 1983). Usually, the mineral is euhedral to subhedral in shape and coarse-grained, measuring up to 5 mm across, and shows various modes of occurrence. Some euhedral grains are intimately intergrown with gersdorffite II, and in some grains abundant lamellae of löllingite II, which exhibit preferred orientation with respect to grain shape may be encountered (see Fig. 5 in a previous paper by Choi and Imai, 1985). In some copper ores rich in chalcopyrite, it forms outer rim around the narrow layer of late magnetite (Mt II) surrounding chalcopyrite. In this case, each grain of arsenopyrite II often shows well-developed crystal face against the gangue minerals.

On some occasions, arsenopyrite II contains spindle- and/or wedge-shaped inclusions consisting of both bismuth and bismuthinite, and monominerallic particles of bismuth with longer dimensions of 100 μm. In addition, extremely tiny particles of bismuth less than 10 μm across scatter throughout the base of arsenopyrite II (Fig. 2 (4)).

Arsenopyrite III, S-excess and As-deficient species but having the composition near the stoichiometric FeAsS, occurs in late hydrothermal veins (ores of Type D in Table 1). In veins rich in siderite as a gangue (D_1), occurs as euhedral to subhedral grains (rhombs), up to 1 mm across in size and is intergrown with tetrahedrite, galena and sphalerite (Fig. 2 (5)). On the other hand, in veins rich in chlorite as a gangue (D_2), it is minor in amounts, occurring as euhedral to subhedral grains up to 5 mm across in size, and is intergrown intimately with "primary" monoclinic pyrrhotite, pyrite and sphalerite (Fig. 2(6)).

In polarized reflected-light, these arsenopyrites have white colour with weakly creamy tints and

bireflectance is faint, but is discernible along the grain boundary from creamy white with bluish tints to white with reddish yellow tints. Between crossed polars, they are strongly anisotropic, giving marked colour effects varying with the different attitude of the section. Polishing hardness of these arsenopyrites is higher than those of the associated löllingite, "primary" monoclinic pyrrhotite and magnetite, and lower than that of pyrite. It decreases considerably with decreasing sulphur contents (arsenian trend). No significant difference is recognizable in their optical properties among arsenopyrites I, II and III. Single crystals of arsenopyrites II and III are also optically homogeneous; no optical zoning is observed.

In this study, the distinction between hexagonal and monoclinic phases of pyrrhotite was made by X-ray diffractometry and Bitter's colloidal suspension method using a magnetite colloid.

ANALYTICAL METHODS

Chemical analysis

Chemical analyses, both qualitative and quantitative were performed with electron microprobe operated in a wavelength dispersion mode (WDX). In this study, the JEOL "JXA-733 Superprobe" with three-channel detecting system and a 40° X-ray take-off angle was used for qualitative analysis (photographing back-scattered electron (compositional and X-ray scanning images), and the "JXA-50A XMA" with two-channel detecting system and a 35° X-ray take-off angle for quantitative chemical analysis, both machines being settled in Waseda University.

The qualitative microprobe analysis by spectrometer scans detected the elements of Ni, Fe, Co, S and As, and rarely Sb. Other elements such as Bi, (Sb) were in most cases less than the sensitivity limits of microprobe; they were not detected even by the careful peak search of the characteristic X-rays.

The instrumental settings of the "JXA-50A" for X-ray intensity measurements in quantitative microprobe analysis were as follows; X-ray excitation voltage; V_o=20 kV, absorption specimen current: i_{ab}=10 nA on MgO, size of electron beams on specimen surface: 1~3 μm, method of X-ray intensity measurement: fixed-time counting mode, the preset of periods of time was 10 sec. Analyzing crystals and characteristic X-rays employed were; LiF for NiKα-, FeKα-, CoKα- and AsKα-lines and PET for SKα- and SbLα-lines. Reference standards utilized were; synthetic NiS for Ni, FeS for Fe and S, pure metal for Co, extra-pure single crystals of InAs and GaAs (impurities less than 10^{-7} ppb) for As, and natural SbAsS for Sb. Special attentions were paid to an analysis for arsenic, the As contents were always checked using the above two extra-pure standards.

After the correction for dead time and background, matrix effects corrections were made with reference to atomic number, absorption and fluorescence (ZAF corrections) and calculation was performed by BASIC computer program "ZAFSU" originally written by Yui and Shoji (1976) with high-speed digital computer system.

X-ray diffraction analysis

The 131 reflection on the X-ray powder-diffraction patterns of arsenopyrite has sufficiently strong intensity and separates well from most interfering peaks of the extraneous materials, and since it appears in a relatively high 2θ-region (FeKα : 72.6°~73.1°), the d-spacings may be measured precisely.

Morimoto and Clark (1961) have shown that the variation in the peak position of the 131 reflection of arsenopyrites is a sensitive indicator of its chemical composition, atomic percent As; and they have given the following relation-

ship,

$$d_{131}\ (\text{Å}) = 1.6006 + 0.00098\ \text{As (atomic percent)} \quad (1a)$$

in another expression we obtain,

$$\text{As (atomic percent)} = 1,020.4\ d_{131}(\text{Å}) - 1,633.27 \quad (1b)$$

Equations (1a) and (1b) are, however, based upon few analyses. Paying an attention to this respect, Kretschmar and Scott (1976) subsequently attempted to refine this linear relationship and proposed the following equation,

$$\text{As (atomic percent)} = 832.08\ d_{131}(\text{Å}) - 1,324.70 \quad (2)$$

There are some discrepancies between Eqs. (1b) and (2).

In order to determine the bulk chemical composition of the Ulsan arsenopyrites II and III, *d*-spacings of the 131 reflection were measured with X-ray diffractometer (Rigaku "Geigerflex", 2026), employing Fe$K\alpha$-radiation by use of Mn-filter and graphite monochromator (λ=1.9373 Å), and reagent-grade CdF_2 as an external standard. The *d*-spacing of the 311 reflection of CdF_2 was calculated to be at 1.6250 Å from the unit-cell edge of 5.3895 (1) Å at 25°C (ASTM Cards, 23-864). The 2θ-region (Fe$K\alpha$) from 72° to 74° was carefully scanned by repetition at least six times with a scanning speed of 1/4 (2θ)/min. and a chart speed of 2 cm/min. Arsenic contents in arsenopyrites were determined by the calculation using Eq. (2).

Prior to X-ray diffractometry, preliminary microprobe analysis was made and arsenopyrite grains containing more than 1 weight percent (Ni+Co) were rejected; i. e., only those with iron contents from 34.0 to 32.0 atomic percent Fe were selected. Moreover, compositional heterogeneity within single grains of arsenopyrites were checked not only by the careful observation of back-scattered electron and X-ray scanning images, but also by that of the linear-scanning profiles for characteristic X-rays obtained by electron microprobe traverses, and the grains with compositional heterogeneity were rejected. As a result, arsenopyrite I has not been subjected to an X-ray diffractometry.

CHEMICAL COMPOSITION

Nineteen analytical data for arsenopyrite I are plotted into enlarged parallerogram in the Ni-Fe-Co triangle diagram as shown in Fig. 3, and the selected microprobe analyses are listed in Table 2 ((1)~(5)), indicating its wide variation in the (Ni+Co) contents with different grains. The maximum (Ni+Co) content attains 10.04

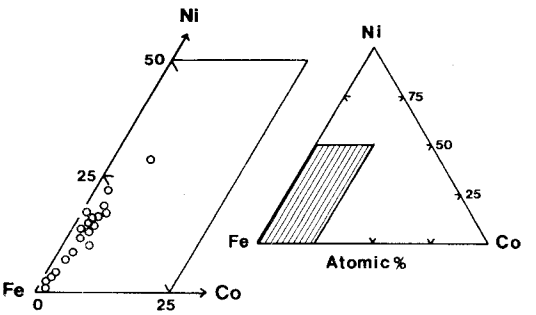

Fig. 3 Enlarged parallerogram in the Ni-Fe-Co triangle diagram, showing the compositional variation of arsenopyrite I with metals.

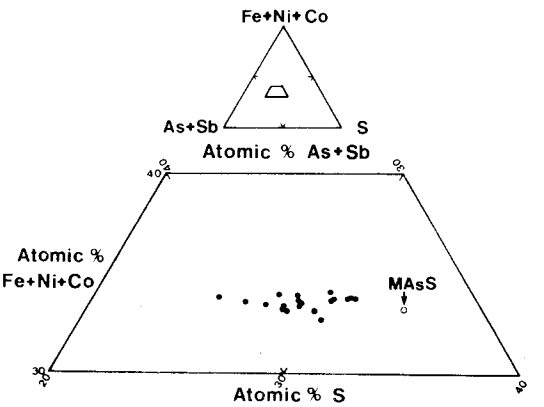

Fig. 4 Enlarged isoscales quadrangle in the (Fe+Ni+Co)-(As+Sb)-S triangle, showing the variation of (As+Sb)/S atomic ratio in arsenopyrite I.
Open circle represents the stoichiometric composition of arsenopyrite, MAsS. M=$\sum$metals.

Table 2 Selective electron microprobe analyses of arsenopyrites from the Ulsan mine.

	Weight percent							Atomic percent					
	Fe	Ni	Co	As	Sb	S	Total	Fe	Ni	Co	As	Sb	S
1	24.86	7.38	0.93	52.90	0.10	14.07	100.24	25.69	7.26	0.91	40.76	0.05	25.33
2	27.08	5.88	0.14	51.34	0.03	15.51	99.98	27.60	5.70	0.14	39.01	0.01	27.54
3	27.26	5.01	1.15	49.42	0.02	16.27	99.13	27.73	4.85	1.11	37.47	0.01	28.83
4	22.30	10.04	2.45	50.50	0.06	16.55	101.90	22.15	9.49	2.31	37.39	0.03	28.64
5	31.74	1.62	0.48	48.44	0.00	17.37	99.65	31.71	1.54	0.45	36.07	0.00	30.23
6	34.51	0.13	0.05	48.35	0.00	18.11	101.15	33.74	0.12	0.05	35.24	0.00	30.85
7	33.94	0.00	0.00	47.36	0.00	18.34	99.64	33.54	0.00	0.00	34.89	0.00	31.57
8	33.56	0.00	0.60	46.95	0.00	18.29	99.40	33.23	0.00	0.56	34.66	0.00	31.55
9	34.22	0.00	0.43	47.08	0.00	18.93	100.66	33.32	0.00	0.40	34.17	0.00	32.11
10	34.69	0.00	0.07	47.16	0.00	19.02	100.94	33.66	0.00	0.07	34.12	0.00	32.15
11	34.77	0.00	0.00	47.21	0.00	19.15	101.13	33.65	0.00	0.00	34.06	0.00	32.29
12	34.72	0.00	0.21	46.49	0.00	19.05	100.47	33.79	0.00	0.19	33.73	0.00	32.29
13	34.58	0.00	0.00	45.67	0.00	19.30	99.55	33.82	0.00	0.00	33.30	0.00	32.88
14	34.60	0.00	0.00	45.76	0.00	19.77	100.13	33.54	0.00	0.00	33.07	0.00	33.39
15	34.91	0.00	0.00	44.45	0.00	20.96	100.32	33.39	0.00	0.00	31.69	0.00	34.92
16	34.68	0.00	0.00	44.23	0.00	21.05	99.96	33.24	0.00	0.00	31.61	0.00	35.15
17	35.58	0.00	0.00	44.35	0.00	20.96	100.89	33.84	0.00	0.00	31.44	0.00	34.72
18	35.18	0.00	0.00	43.25	0.00	21.24	99.67	33.69	0.00	0.00	30.88	0.00	35.43
19	35.36	0.00	0.00	42.56	0.00	21.75	99.67	33.68	0.00	0.00	30.22	0.00	36.09
20	35.69	0.00	0.00	42.20	0.00	22.20	100.09	33.73	0.00	0.00	29.73	0.00	36.55

1~5: Arsenopyrite I. 6~14: Arsenopyrite II. 15~20: Arsenopyrite III.
1: Specimen No. 532. 2~3: Specimen No. 338. 4: Specimen No. 532 (core). 5: Specimen No. 532 (rim). 6: Specimen No. 316. 7: Specimen No. 807. 8: Specimen No. 1022. 9: Specimen No. 733. 10: Specimen No. B8103-3. 11: Specimen No. B8102-2. 12: Specimen No. 106. 13: Specimen No. 101. 14: Specimen No. 820880. 15~16: Specimen No. 600. 17: Specimen No. 709. 18~20: Specimen No. B8004-4.

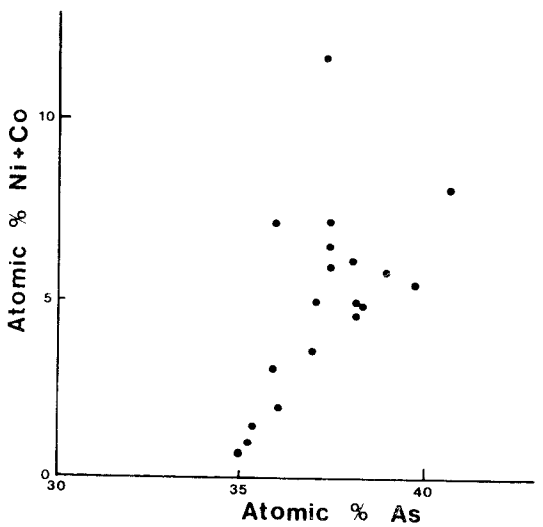

Fig. 5 The relation between atomic percent (Ni+Co) and atomic percent As in arsenopyrite I.

Ni, 2.45 Co (in weight percent) in the core of a single crystal that has compositional zoning.

In Fig. 4, the analytical data are plotted into a central portion of the triangle diagram of (Fe+Ni+Co)—(As+Sb)—S, showing that arsenopyrite I is an As-excess and S-deficient species of high-temperature type. Also, Fig. 5 shows the variations in a atomic percent (Ni+Co) versus atomic percent As for arsenopyrite I, from which it may be seen that, with increasing (Ni+Co) content the As content increases in approximately linear fashion (arsenian trend).

In a preceding chapter of this paper, it was already pointed out that the compositional zoning of arsenopyrite I might be recognized. Figure 6 (A) gives the back-scattered electron image and

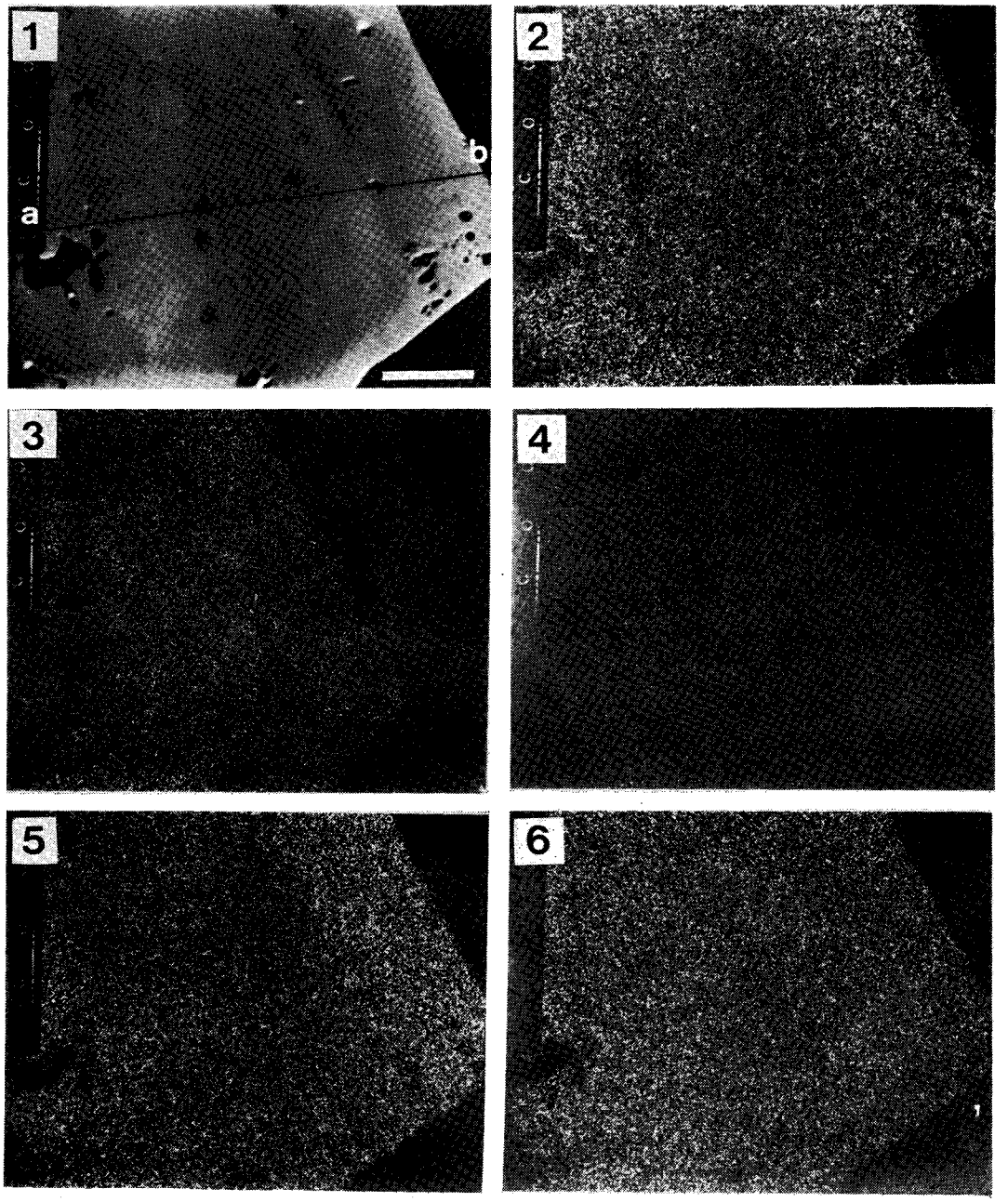

Fig. 6(A) Back-scattered electron image and X-ray scanning images, showing the compositional zoning in arsenopyrite I.

the corresponding X-ray scanning images from NiKα-, FeKα-, CoKα-, SKα-, and AsKα-radiations, and (B) shows the linear scanning profiles from these characteristic X-rays. These figures clearly shows the compositional zoning with (Ni, Co)- rich core(10.04 Ni, 2.45 Co in weight percent) and (Ni, Co)-poor rim within single grain. They also indicate that core has a higher content in As than the rim.

Selected microprobe analyses of arsenopyrite

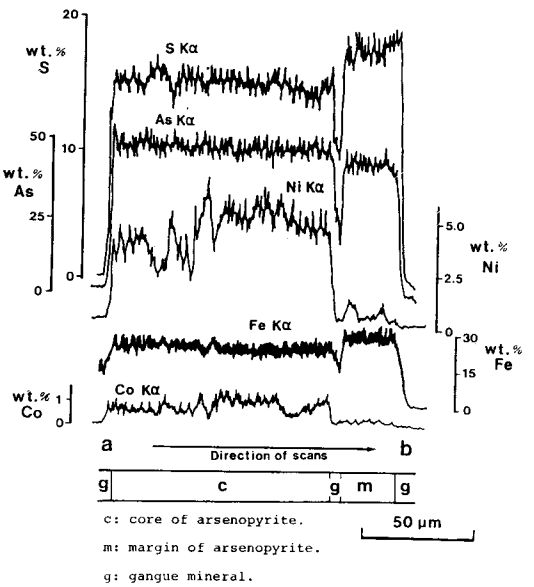

Fig. 6(B) The linear-scanning profiles from characteristic X-rays along the line a—b marked in Fig. 6(A)-(1).

II are listed in Table 2 ((6)～(14)), indicating that it also represents an As excess and S-deficient species of high-temperature type, despite the negligible contents in (Ni+Co). On the contrary, arsenopyrite III in Table 2 ((15)～(19)) shows its As-deficient and S-excess species of low-temperature type, though it has the composition close to stoichiometric FeAsS.

It has been shown elsewhere (e.g., Kretschmar and Scott, 1976) that arsenopyrite has various proportion of As within single grains, but so far as arsenopyrites II and III from the Ulsan mine are concerned, except for few instances (Imai and Choi, 1984), no such a compositional heterogeneity is recognizable not only in the linear-scanning profiles from AsKα-radiation obtained by electron microprobe traverses, but also in the results of multiple spot analyses in single crystals within the precision of microprobe analytical level (±0.35 atomic percent As).

Table 3 shows bulk chemical composition (As and S contents) of arsenopyrites II and III, which come from the ores with various mineral assemblages, calculated from the 131 peak positions as determined by X-ray diffractometry toge-

Table 3 The d_{131}-spacing(Å) and As contents of arsenopyrites II and III from the Ulsan mine and the associated ore minerals.

	Specimen No.	d_{131}(Å)	N*	As** atomic %	As*** atomic %	N****	Associated ore minerals
1	US-316	1.6338±1	7	34.8±0.1	35.5±0.3	5	gf, mo, bi, lo
2	807	1.6335±3	6	34.6±0.3	35.0±0.8	7	bi
3	1022	1.6335±1	7	34.6±0.1	34.8±0.5	9	lo, bi
4	733	—	—	—	34.5±0.3	5	mt, lo, bi
5	8102-2	1.6331±2	8	34.3±0.2	34.4±0.5	3	lo, bi
6	106	1.6327±2	9	33.9±0.2	34.0±0.4	9	bi, bm
7	81-3-3	—	—	—	33.9±0.6	5	bi
8	101	1.6327±1	8	33.9±0.1	33.8±0.8	9	bi, bm
9	820880	1.6333±2	7	34.4±0.2	33.6±0.7	9	mt, sh, cp, lo, cb, sp, bo, bi, rq, td
10	709	1.6309±3	8	32.3±0.2	32.1±0.6	7	po, cp, sp, mo
11	600-A	—	—	—	32.1±0.5	14	py, sp, gl, mc, pg, td
12	8004-A	—	—	—	30.2±0.6	10	py, gl, sp, mc

*Number of individual determinations by X-ray diffractometry. **Calculated values from the equation given by Kretschmar and Scott(1976), Eq. (2) in this paper. ***Average of atomic percent As as determined by electron microprobe. ****Number of spot analyses by electron microprobe.
1～9: arsenopyrite II, 10～12: arsenopyrite III.
Abbreviations of associated ore minerals: bi=bismuth, bm=bismuthinite, bo=bornite, cb=cubanite, cp=chalcopyrite, gf=gersdorffite, gl=galena, lo=löllingite, mc=marcasite, mo=molybdenite, mt=magnetite, pg=pyrargyrite, po=pyrrhotite, py=pyrite, rq=roquesite, sh=scheelite, sp=sphalerite, td=tetrahedrite.

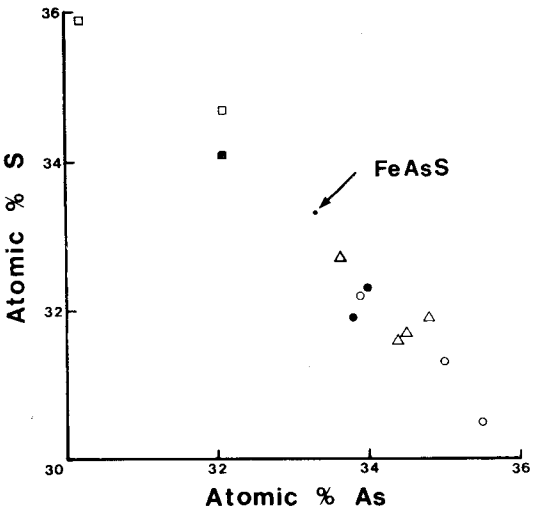

Fig. 7 Variation of atomic percent As as related to mineral assemblage in arsenopyrites II and III.
Open circle: bismuth+arsenopyrite II, full circle: bismuth + bismuthinite + arsenopyrite II, open triangle: bismuth+löllingite+arsenopyrite II, open square: pyrite+arsenopyrite III, full square: pyrrhotite+arsenopyrite III.

ther with the average As contents obtained by multiple spot microprobe analyses. The results are also plotted into the diagram showing the variation of the compositions as expressed by atomic percent As versus atomic percent S in Fig. 7. These table and figures clearly indicate the approximately linear relationship with negative gradient between arsenic and sulphur contents. Also, it is indicated that arsenopyrite II coexisting with löllingite, bismuth and/or bismuthinite are relatively rich in arsenic and poor in sulphur, whereas arsenopyrite III coexisting with "primary" monoclinic pyrrhotite or pyrite are relatively rich in sulphur and poor in arsenic.

ARSENOPYRITE AS A INDICATOR OF TEMPERATURES AND SULPHUR FUGACITIES—A DISCUSSION

The atomic ratio As/S or atomic percent As of arsenopyrite is very sensitive to sulphur fugacities (activities), $f(S_2)$. When arsenopyrite comes from sulphur-buffer assemblages, however, the composition is mainly a function of temperature as mentioned before. Arsenopyrite having the most refractory nature among the common ore minerals is unlikely to change its composition in response to the subsequent variation of conditions, and this makes it a useful tool for deciphering the physicochemical environments during its crystallization.

Clark (1961) has suggested that the atomic ratio As/S of arsenopyrite decreases with increasing confining pressure (S-rich trend). However, Kretschmar and Scott (1976) have given a pseudobinary T-X diagram along the pyrite-löllingite join based upon their experimental results for the condensed Fe-As-S system. In the low-pressure region, they have ignored the pressure effects on the phase relations, and stressed its role as a geothermometer, provided that minor elements content does not exceed 1 weight percent. These authors have observed significant variation for the atomic ratio As/S of arsenopyrite grains in the same specimen, even though the specimen has a sulphur-buffer assemblage, and they attribute this to the local variation of $f(S_2)$ during its crystallizaion.

Among the Ulsan arsenopyrites with three generations, arsenopyrite I is not permitable for a geothermometer, because the (Ni+Co) content always exceeds 1 weight percent.

Kretschmar and Scott (1976) cited an occurrence of the mineral assemblage, bismuth+bismuthinite+sphalerite+arsenopyrite in veins of the Mount Pleasant mine (now Brunswick Tin Mine Ltd.), Canada (Petruk, 1964) and pointed out that composition of arsenopyrite might serve as a geothemometer, despite the absence of Fe-S minerals. To the present author's knowledge, however, no examination of the Mount Pleasant material as a geothermometer seems to have been

made so far.

At Ulsan, arsenopyrite II occasionally contains inclusions consisting both bismuth and bismuthinite as mentioned before. The equilibrium between bismuth (melt, Bi(l)) and bismuthinite may be described by the following equation.

$$4/3\ \mathrm{Bi}(l)+\mathrm{S_2}=2/3\ \mathrm{Bi_2\ S_3} \qquad (3)$$

The $1/T-f(\mathrm{S_2})$ relationship in Eq. (3) may be estimated from the following Eq. (4) given by Craig and Barton (1973) combining with familiar equations (Eqs. (5) and (6)).

$$\Delta G^0=-55,600+42.60T \quad (271\sim450\ ^\circ\mathrm{C}) \qquad (4)$$

$$\Delta G^0=-RT\ln K \qquad (5)$$

$$\ln K=(2.303)\cdot[-\log f(\mathrm{S_2})] \qquad (6)$$

where ΔG^0 refers to standard Gibbs energy change of reaction in Eq. (3), (cal.), R denotes the gas constant, K equilibrium constant at definite temperature and T temperature in K. Above 450 °C, the relation of Eq. (4) is no longer linear, but valid thermochemical data published are not available, accordingly the Bi (l) $-\mathrm{Bi_2\ S_3}$ buffer-curve above this temperature in Fig. 8 is drawn following that given by Barton and Skinner (1967).

Fig. 8 is obtained by superimposing the above $1/T$-$f(\mathrm{S_2})$ relationship upon the diagram given by Kretschmar and Scott (1976), showing the phase relation for the Fe-As-S system in equilibrium with vapour.

As can be seen in Fig. 8, the Bi(l)—$\mathrm{Bi_2\ S_3}$ sulphur-buffer univariant curve thus drawn lies within the arsenopyrite stability field and intersects its isopleths at sufficiently large angle, constituting a potentially useful geothermometer. Since each isopleth is univariant at a definite pressure, their intersections are invariant, defining not only temperature, but also unique $f(\mathrm{S_2})$. As listed in Table 3, the As contents of arsenopyrite coexisting with bismuth and bismuthinite range from 33.8 to 34.0 atomic percent As. This corresponds to the temperature range between 460 and 470 °C and the $\log f(\mathrm{S_2})$ range between −7.4 and −7.0, based upon the assumption that arsenopyrite+bismuth+bismuthinite is equilibrium assemblage.

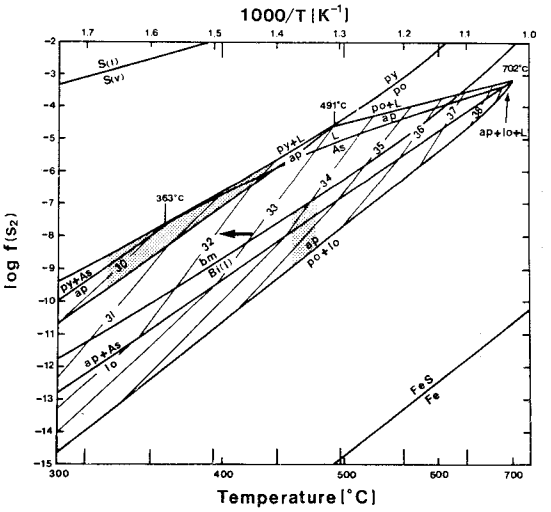

Fig. 8 Sulphur fugacity-temperature projection of the stability field of arsenopyrite given by Kretschmar and Scott (1976), upon which bismuth (melt)-bismuthinite buffer curve is superimposed.
Number of isopleths indicates the atomic percent As in arsenopyrite. Abbreviations; ap= arsenopyrite, As=arsenic, bi=bismuth (melt, l), bm=bismuthinite, L=liquid, lo=löllingite, po = pyrrhotite, py = pyrite. Sulphur fugacity is expressed in logarithmic terms.

The composition of arsenopyrite II coexisting with löllingite and bismuth in some cases, representing the common mineral assemblage in the Ulsan arsenic ores does not serve as a geothermometer, because the löllingite-(arsenic+arsenopyrite) buffer curve in Fig. 8 cannot be operative due to the lack of arsenic phase or to the absence of evidence to show the existence of excessive arsenic. Moreover, within the löllingite +arsenopyrite field, the slope of isopleths of arsenopyrite in Fig. 8 becomes abruptly gentle, accordingly neither temperature nor $f(\mathrm{S_2})$ is constrained. However, textural study by ore microscopy indicates that, though the formation of arsenopyrite II continued after the ceasing of

crystallization of löllingite II as shown in Fig. 1, the two minerals might be regarded as products of approximately contemporaneous crystallization. Consequently, it may be reasonably assumed that the difference in mineral assemblages of the ore specimens might depend mainly upon the local variation of $f(S_2)$, having a tendency to increase slightly in time evolutional trend rather than temperature. Based upon the above assumptions, the possible $1/T$-$f(S_2)$ field of arsenopyrite II may be expressed by the shaded area on the right hand in Fig. 8.

With respect to arsenopyrite III in ore Type D_1 from the latest hydrothermal veins coexisting with galena and sphalerite provides restricted limits for neither temperature nor $f(S_2)$, and only arsenopyrite III coexisting with pyrite and "primary" monoclinic pyrrhotites in ores of Type D_2 is available for a geothermometer. As shown in Table 3, the arsenic contents of arsenopyrite III coxisting with pyrite vary from 30.2 to 32.1 atomic percent As. This corresponds to the temperature range from 320 to 440 °C and the log $f(S_2)$ range from −9.0 to −7.0 as indicated by the shaded area on the left hand in Fig. 8.

CONCLUDING REMARKS

The present study shows compositional variation in three arsenopyrites I, II and III with different generation from the Ulsan arsenic and polymetallic ores, and evaluates the use of geothermometer. Unfortunately, in the present ores the sulphur-buffer assemblage pyrite+hexagonal pyrrhotite+arsenopyrite, which may be encountered commonly in sulphide ores is not recognized, however, the presence of bismuth (*l*)-bismuthinite buffer enables arsenopyrite II successfully to the estimation of either temperature or sulphur fugacity.

As shown in Fig. 8, the chemical contrast between arsenopyrites II and III may be ascribed to the variation of temperature rather than sulphur fugacity. Fluid inclusion study on late grandite garnets with optically anisotropic nature, which is somewhat earlier than arsenopyrite II, indicates that the homogenizing temperature of primary fluid inclusions ranges from 400 to 450 °C and the salinity ranges from 16.9 to 22.2 weight percent equivalent NaCl (Choi, 1983). After the pressure and salinity corrections for the homogenizing temperature, the formation temperature may be estimated in the range from 430 to 470 °C. This is compatible with the temperature data for arsenopyrite II as described before.

Referring to the experimental investigation on the stability relation of siderite in the system Fe-C-O given by French (1971), Choi (1983) determined the following temperature and oxygen fugacity, $f(O_2)$ during the formation of siderite, representing the dominant gangue mineral and the latest crystallization in ores of Type D_1 from hydrothermal veins. Nemely, temperature ranges from 280 to 330 °C and $\log f(O_2)$ from −35 to −30 on the basis of the assumption that $P_{Total}=P_{H_2O}+P_{CO_2}=0.5$ kb and $X_{CO_2}=0.05\sim0.1$. These results are also consistent with temperature data for arsenopyrite III in ores of Type D_1, ranging from 320 to 440 °C as mentioned before. Probably, formation of the vein initiated at temperatures higher than 300 °C and terminated at about 280 °C.

At the beginning of this paper, geological environments during the formation of the Ulsan ore deposits are considered in relation to regional and local geologic-settings, and the physicochemical conditions are suspected to some degrees, in particular the formation pressure is fixed at 0.5 kb (50 MPa). However, this premise does not bring about any contradictions against the present study on arsenopyrite geothermometry. It is emphasized here that, laboratory works for geothermometry must be made on the minerals, the position of which is clear in both time and

space.

Recently, Scott (1983) has proposed the diagram of $\log f(S_2)$ versus $1,000/T$, K for sphalerite and arsenopyrite in equilibrium with hexagonal pyrrhotite and/or pyrite and stated that the composition of these two minerals can provide reliable temperature and $f(S_2)$ during the ore-forming process in low pressure region, provided that the ore specimens are cooled rapidly to prevent from retrograde reaction. In the present study, no examination in this respect has been made. Further intensive study on the Ulsan polymetallic ores seems desirable.

ACKNOWLEDGEMENTS

We wish to express our sincere thanks to Professor S. C. So of Korea University, and Professor T. Mariko and Drs. Y. Ogasawara and E. Uchida of Waseda University, Japan for their kind advice and critical reading of this paper in manuscript. Thanks are also due to Professors H. Ozaki and I. Ohdomari of Waseda University for their kind presentation of extra-pure single crystals of InAs and GaAs for microprobe standards of arsenic. We are grateful to officials of the Ulsan mine, especially to Mr. J. H. Lee, General Manager, for their warmful assistance during our field works.

We are indebted to the Computer Centre of the University of Tokyo and Remote Data Station (RDS) of Waseda University for the access of high-speed digital computer, HITAC M280/M200/S801 system in the computation for the ZAF corrections of microprobe data (Project No. 035643002).

This study was financially supported in part by a Grant-in-Aid for Specified Research Project ("Tokutei Kadai Kenkyu Joseihi"), 1983/1984, Grant No. 58B-22 from Waseda University awarded to one of us (N.I.), to which we are grateful.

REFERENCES

Barton, P.B. and Skinner, B.J. (1967) Sulphide mineral stabilities. In: H.L. Barnes (ed.) Geochemistry of Hydrothermal Ore Deposits. Holt, Rinehart and Winston, New York, p.236-333.

Berglund, S. and Estrom, T.K. (1980) Arsenopyrite and sphalerite as T-P indicators in sulphide ores from northern Sweden. Miner. Deposita, v.15, p.175-187.

Chang, K.H. (1975) Cretaceous stratigraphy of southeast Korea. Jour. Geol. Soc. Korea, v.11, p.1-23.

Choi, H.I., Oh, J.H., Shin, S.C. and Yang, M.Y. (1980) Geology and geochemistry of the Gyeongsang strata in Ulsan area (in Korean with English abstr.). Korea. Res. Inst. Geosci. Miner. Resources Bull., no.20, p.1-33.

Choi. S.G. (1983) Skarn evolution, and iron-tungsten mineralization and the associated polymetallic mineralization at the Ulsan mine, Republic of Korea. Ph. D. Thesis submitted to the Graduate School of Science and Engineering, Waseda University, No. Koh 627, 271p.

Choi, S.G. and Imai, N. (1983) Miharaite in bornite-rich copper ore from the Ulsan mine, Republic of Korea. Jour. Japan. Assoc. Miner. Petrolog. Econ. Geol., v.78, p.350-360.

Choi, S.G. Imula, K. and Imai, N. (1983) Occurrence and chemical composition of green garnet from the Ulsan mine, Republic of Korea. Jour. Japan. Assoc. Miner. Petrolog. Econ. Geol., v.78, p.428-440.

Choi, S.G. and Imai, N. (1985) Ni-Fe-Co arsenides and sulpharsenides from the Ulsan mine, Republic of Korea. Mining Geol., v.35, p.1-16.

Choi, S.G., Chung, J.I. and Imai, N. (1985) Compositional variation of arsenopyrites in polymetallic ores from the Ulsan mine, Republic of Korea, and their application to a geothermometer (abstr. in Japanese). Coll. Abstr. Autumn Joint Meet. MSJ, SMGJ and JAMPE, C-35, p.134.

Clark, L.A. (1960) The Fe-As-S system. Phase relations and application. Econ Geol., v.55, Part I: p.1345-1381, Part II: p.1631-1652.

Craig, J.R. and Barton, Jr. (1973) Thermochemical

approximations for sulfosalts. Econ. Geol., v.68, p.493-506.

Dewitt, D.B. and Essene, E.J. (1974) Sphalerite geobarometry applied to Greenville marbles (abstr.). Geol. Soc. Amer. Abstr. with program 6, p.709-710.

French, B.M. (1971) Stability relations of siderite ($FeCO_3$) in the system Fe-C-O. Amer. Jour. Sci., v.271, p.37-78.

Imai, N. and Lee, H.K. (1980) Complex sulphide-sulphosalt ores from the Janggun mine, Republic of Korea. In Complex Sulphide Ores, Proc. Internat'l. Conf. on Complex Sulphide Ores, p.248-259.

Imai, N. and Choi, S.G. (1983) Origin of calcite gigantic crystals in the "abnormal calcite zone" at the Ulsan mine, Republic of Korea (abstr. in Japanese). Mining Geol., v.33, p.48-49.

Imai, N. and Choi, S.G. (1984) The first Korean occurrence of roquesite. Miner. Jour., v.12, p.162-172.

Ishihara, S., Lee, D.S. and Kim, S.Y. (1981) Comparative study of Mesozoic granitoids and related W-Mo mineralization. Mining Geol., v.31, p.311-320.

Jin, M.S., Kim, S.Y. and Lee, J.S. (1981) Granitic magmatism and associated mineralization in the Gyeongsang Basin, Korea. Mining Geol., v.31, p.245-260.

Kretschmar, U. and Scott, S.D. (1976) Phase relations involving arsenopyrite in the system Fe-As-S and their application. Canad. Miner., v.14, p.364-386.

Lee, Y.J. and Ueda, Y. (1977) K-Ar dating on granitic rocks from Eonyang and Ulsan areas, Korea (in Japanese with Engilish abstr.). Jour. Japan. Assoc. Miner. Petrolog. Econ. Geol., v.72, p.367-372.

Lusk, J., Campbell, F.A. and Krouse, H.R. (1975) Application of sphalerite geobaromety and sulphur isotope geochemistry to ores of the Quemont mine, Nevada, Quebec. Econ. Geol., v.70, p.1070-1083.

Morimoto, N. and Clark, L.A. (1961) Arsenopyrite crystal-chemical relations. Amer. Miner., v.46, p.1448-1469.

Park, K.H. and Park, H.I. (1980) On the genesis of Ulsan iron-tungsten deposits (in Korean with English abstr.). Jour. Korean Inst. Min. Geol., v.13, p.104-116.

Park, Y.D. and Yoon, H.D. (1968) Explanatory Text of the Geological Map of Ulsan Sheet (in Korean with English abstr.). Geol. Surv. Korea, p.1-20.

Petruk, W. (1964) Mineralogy of the Mount Pleasant tin deposits in New Brunswick. Mines Branch Tech. Bull., TB56, Dept. Energy Mines Res., Ottawa, 35p.

Scott, S.D. and Barnes, H.L. (1971) Sphalerite geothermometry and geobarometry. Econ. Geol., v.66, p.653-669.

Scott, S.D. (1983) Chemical behaviour of sphalerite and arsenopyrite in hydrothermal and metamorphic environments. Miner. Mag., v.47, p.427-435.

蔚山鑛山産 硫砒鐵石의 組成變化 및 地質溫度計에 對한 適用

崔 善 奎·鄭 在 一·今 井 直 哉

요약：蔚山의 철·중석 스카른광상에서 산출되는 硫砒鐵石은 그의 産出狀態·鑛物共生關係·化學組成을 근거로 세가지 유형으로 구분된다. 硫砒鐵石 Ⅰ은 多金屬鑛化作用 초기에 정출된 것으로 주로 스카른대 내에서 산점상으로 분포하며, Ni-Fe-Co계 유화물과 밀접한 공생관계를 보여준다. 硫砒鐵石Ⅰ의 화학조성은 Ni, Co의 함량이 현저하게 높고 As/S(原子比)>1으로 過剩의 비소를 함유한다. 硫砒鐵石Ⅱ는 Cu 또는 As 광석중에서 산출되며, 비독사석·휘창연석·비스무스·황동석·섬아연석과 밀접한 공생관계를 보여준다. 硫砒鐵石Ⅱ의 화학조성은 Ni, Co의 함량이 극히 미량이며, As/S>1으로 過剩의 비소를 함유한다. 硫砒鐵石Ⅲ은 최후기 열수광맥 형성시기에 정출되었으며, 황철석·방연석·섬아연석·자류철석과 밀접한 共生關係를 보여준다. 硫砒鐵石Ⅲ의 化學組成은 As/S≦1로 過剩의 S를 함유한다. 硫砒鐵石 Ⅰ은 Ni, Co의 함유량이 1%이상이므로 地質溫度計로 사용할 수 없지만, 硫砒

鐵石Ⅱ는 비스무스-휘창연석의 共生關係를 보여 주고 있으므로, 이를 Kretschmar and Scott(1976)에 의한 $1/T$—$f(S_2)$도에 적용시켜보면 硫砒鐵石Ⅱ의 정출환경은 T=460～470°C, log $f(S_2)$=−7.4～7.0이고, 硫砒鐵石Ⅲ의 정출환경은 T=320～440°C, log $f(S_2)$=−9.0～7.0으로 추정된다.

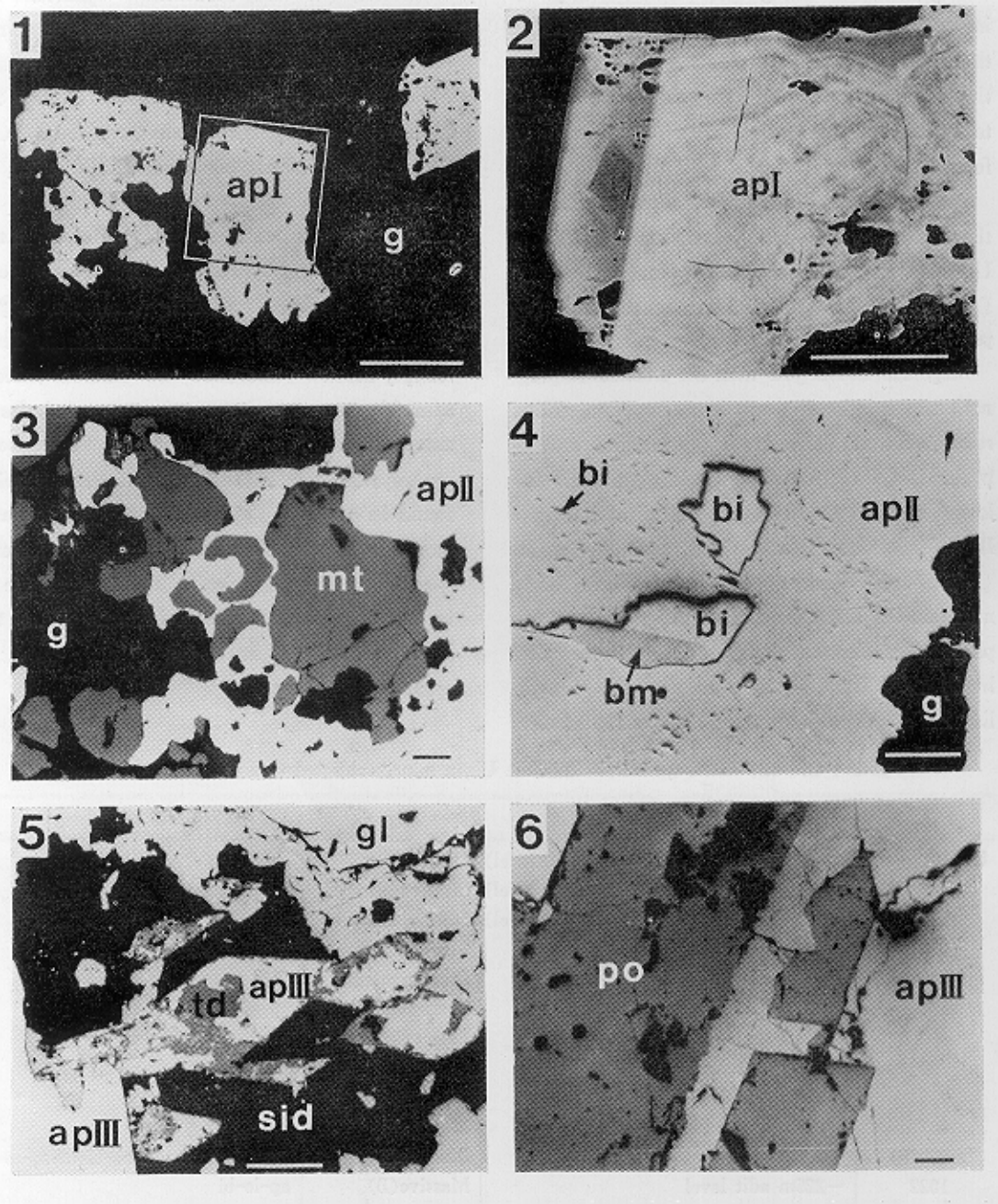
1
apI
g
2
apI
3
apII
mt
g
4
bi
bi
apII
bi
bm
g
5
gl
apIII
td
apIII
sid
6
po
apIII

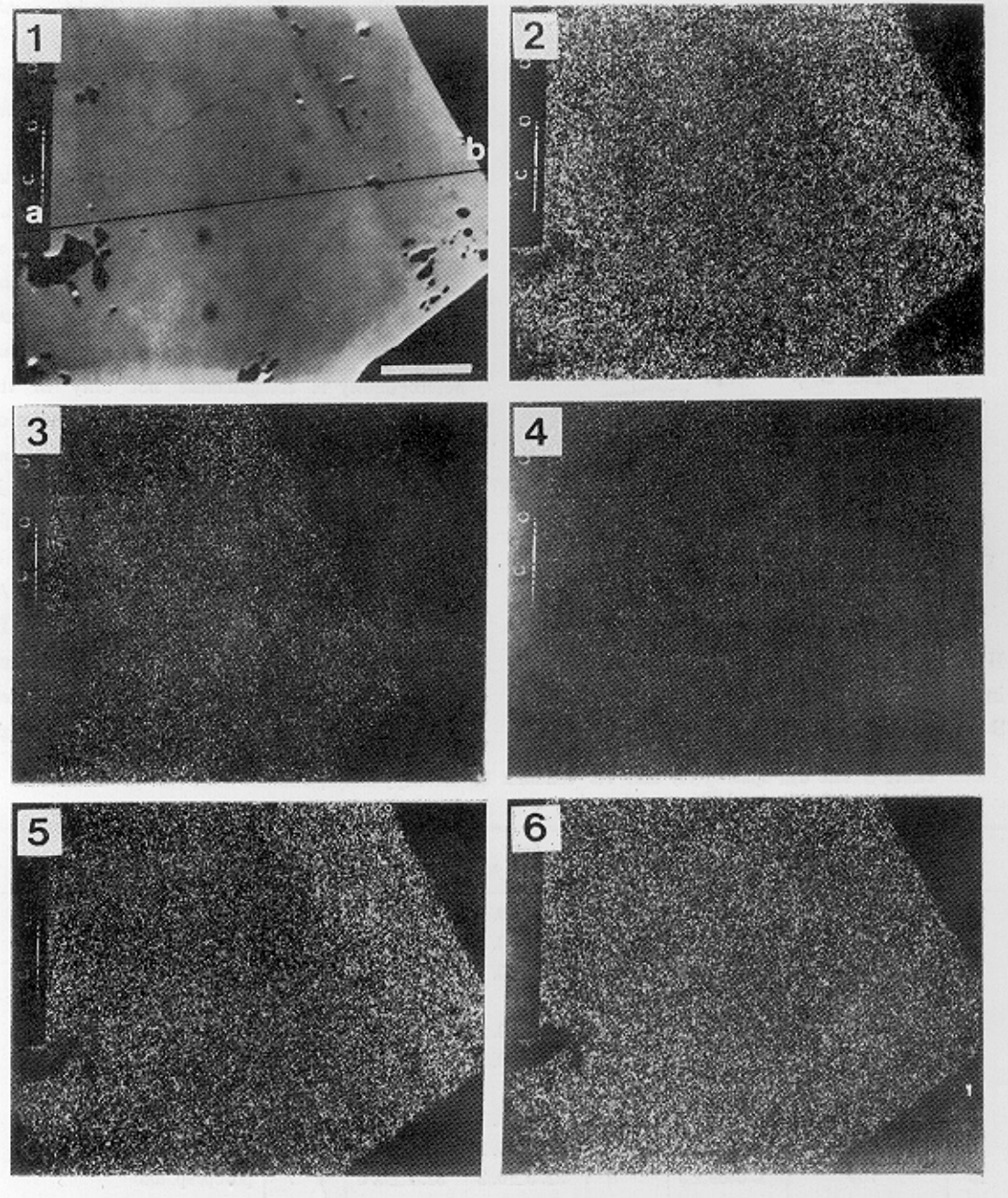
1
a
b
2
3
4
5
6